Dissipative neurodynamics in perception forms cortical patterns that are stabilized by vortices

Walter J Freeman[1] **and Giuseppe Vitiello**[2] [3]

[1] Department of Molecular and Cell Biology University of California, Berkeley CA 94720-3206 USA

[2] Dipartimento di Matematica e Informatica and INFN Universitá di Salerno, I-84100 Salerno, Italy

E-mail: dfreeman@berkeley.edu - http://sulcus.berkeley.edu
vitiello@sa.infn.it - http://www.sa.infn.it/giuseppe.vitiello

Abstract. In the engagement of the brain with its environment, large-scale neural interactions in brain dynamics create a mesoscopic order parameter, which is evaluated by measuring brain waves (electrocorticogram, ECoG). Such large-scale interactions emerge from the background activity of the brain that is sustained by mutual excitation in cortical populations and manifest in spatiotemporal patterns of neural activity. Band pass filtering reveals beats in ECoG power that recur at theta rates ($3-7$ Hz) as null spikes in $\log_{10}$ power. The order parameter transiently approaches zero, and the microscopic activity is both disordered and symmetric. As the null spikes terminate, the order parameter resurges and imposes a mesoscopic spatial pattern of ECoG amplitude modulation that then governs the microscopic gamma activity and retrieves the memory of a stimulus. The brain waves reveal a spatial pattern of phase modulation in the form of a cone. The dissipative many-body model of brain dynamics describes these phase cones as vortices, which are initiated by the null spikes, and which stabilize the amplitude modulated patterns embedded in the turbulent neural noise from which they emerge.

1. Introduction

In 1958 von von Neumann observed that the operations performed by the brain are not done with logic and mathematics: "Brains lack the arithmetic and logical depth that characterize our computations... We require exquisite numerical precision over many logical steps to achieve what brains accomplish in very few short steps" (p. 63 of ref. [1]). Schematically, we might identify three of such steps. The brain provides guidance for the engagement of the body with its environment, which requires constant attention and control with the various senses. The first step in perception thus consists in the transduction of microscopic energies from the surroundings at sensory receptors that expresses the information in action potentials (nerve impulses). The acquisition of information about the current status of the body and its surroundings is indeed a necessary step. Then, the rapid recognition of momentary changes to which the body must accommodate and compare at each moment with all relevant past experience in similar conditions is crucial in order to successfully engage the body with its environment. Thus the second step is refinement of the requisite information at a higher resolution in the sensory systems. The third step is abstraction and generalization. Such a step consists in the continual updating of

[3] Corresponding author

the *meaning* of the flow of information exchanged in the brain's behavioral relation with its environment. The brain thus stores *experience*, which constitutes the basis for *knowledge*. The survival of the body in the environment in which it is situated thus crucially depends on the brain *action-perception* cycle, namely the capability of the brain to be *open* on the environment and to react to it. This means that neurodynamics is intrinsically dissipative. Dissipation, i.e. the reciprocal exchange of energy (in various forms of information, matter, radiation, etc.) between the brain and its environment, is a characterizing feature of brain dynamics. Therefore, non-equilibrium processes, critical phenomena, and phase transitions necessarily enter into any realistic modeling of brain function [2, 3].

In this paper we will discuss neurophysiological data from the perspective of dissipative neurodynamics. Nonlinear ordinary differential equations (ODE) in networks called Katchalsky-sets (KI, KII, etc. sets) [4] have been implemented in an analog very large scale integration [5], putting a KII set on a chip with about 800 first order ODE to describe an 8×8 electrode array. This report extends the modeling of the third step into many-body physics [6]. We are motivated in this by the fact that there is no conventional neural network offered by neuroscientists or neuroengineers that can adequately model or simulate our data. In our approach, the cerebral cortex is described as a network of populations that organize into a state of criticality, which has many unitarily inequivalent ground states that constitute memories. Access and retrieval of memories, in the act of recognition, are shown to occur through phase transitions. Retrieved memories are expressed in spatial patterns of amplitude modulation (AM) of carrier frequencies. The AM patterns are stabilized by vortices in the turbulence of cortical background activity in the form of phase cones.

This paper is organized as follows. We will first review neurophysiological data and show how from these some features emerge which point to consider collective dynamical processes in theoretical modeling. We will then review the dissipative model and show its agreement with observations.

2. Comparison of the microscopic sensory recept with the mesoscopic percept

A large part of contemporary neuroanatomy and neurophysiology provides the basis for understanding of the first two steps mentioned above. The understanding of the third step, heretofore unknown, presents difficulties which were clearly stated over fifty years ago by Lashley: "Generalization is one of the primitive basic functions of organized nervous tissue. Here is the dilemma. Nerve impulses are transmitted ... from cell to cell through definite intercellular connections. Yet all behavior seems to be determined by masses of excitation. ... What sort of nervous organization might be capable of responding to a pattern of excitation without limited specialized paths of conduction? The problem is almost universal in the activities of the nervous system" (p. 302-306 of ref.[7]).

This third step is taken in the several sensory cortices that receive the information from receptors. The prototype for all the sensory and perceptual stems in the evolution of mammalian brains is that for olfaction combined with the hippocampal system for memory formation. The functions of the three-layered allocortex in these ancient structures illustrate the elementary mechanisms that transpose from information in sensory input to memory in perception.

The topology of the olfactory system

The topology of the olfactory system is shown schematically in three sequential surfaces: receptors, bulb and cortex. In round figures, there are 10^3 types among the 10^8 receptors giving 10^5 of each type. Any one sniff selects very few of each type, e.g., 10^2, with random variation on successive sniffs owing to nasal turbulence (Fig. 1). Assignment of the sample on each sniff to the class of odors to which it belongs requires inductive generalization. This is done in reinforcement

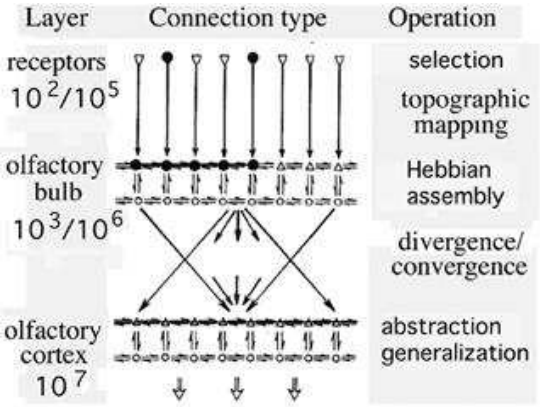

Figure 1. The topology of the olfactory system is schematized in 3 surfaces. In Step 1, receptors transduce an input of chemical energy to nerve impulses. In Step 2, after topographic mapping and convergence, a Hebbian assembly generalizes the input to an odorant class. In Step 3, a mesoscopic AM pattern (Fig. 2) is created by a phase transition. Transmission by a divergent-convergent pathway enacts an integral transformation that abstracts the output, deleting the sensory details.

learning by strengthening of synapses (increased gain, k_{ee}) among bulbar excitatory neurons ('$\bigtriangledown$' in Fig. 1) that are co-activated on each sniff by a reinforced odorant (rewarded or punished). Cumulatively, increases form a Hebbian nerve cell assembly ('$\bullet-\bullet-\bullet-\bullet$') for each learned class by pair-wise correlation on reinforced trials and decorrelation by habituation on sniffs without the reinforcement. Neurons selected by odorant sensing show membership in an assembly by vigorous firing of microscopic impulses. Excitation of any members of the assembly by a learned stimulus activates the entire assembly. However, an assembly only comprises an estimated 0.1% of the excitatory neurons in the bulb, so its activation at the microscopic level does not explain perception. Amplification is required to the entire olfactory bulb at the mesoscopic level. That is done by dendritic integration, which produces continuous fields of gamma neural oscillations that are observed and measured in the olfactory bulbar and cortical electrocorticogram (ECoG). The dynamical formation and spatial extension of these observed fields of neural oscillations are explained by the dissipative many-body model (Section 5).

The transmission from receptors to the bulb is done by topographic mapping, which is compatible with microscopic content (action potentials as point processes); transmission from the bulb to the cortex is done by divergent-convergent projection performing a spatiotemporal integration of the global output of the bulb. The act of integration enhances gamma oscillatory field potentials that share the same instantaneous analytic frequency. It attenuates activity that is spectrally dispersed, including sensory-driven activity, and expresses as output only the activity constructed by the bulb from its updated memory store. The transmission in the step from bulb to cortex is done by action potentials, but the organization differs from the prior step. In the topographic input path to the bulb, the state variable is pulse frequency (Fig. 1); in the output projection from the bulb, the state variable is pulse density. The conversion from microscopic frequency to mesoscopic density is initiated at the input synapses, where pulse frequencies are transduced to dendritic current amplitudes; the conversion is completed at the output synapses of target neurons, by the spatiotemporal integration performed by the divergent-convergent projection. The wave densities of the olfactory bulb ECoG reveal its mesoscopic output, resulting from bulbar dendritic integration prior to the global integral transformation. The cortical ECoG in the third layer reveals the cortical transformation of its bulbar input.

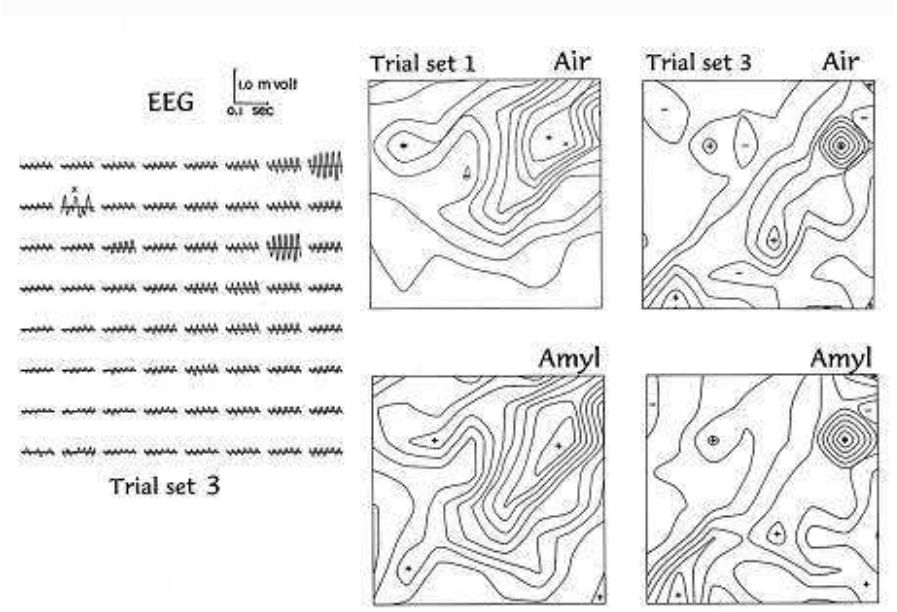

Figure 2. Left: Example of an AM carrier wave in one frame. Center: contour plots of AM patterns from 4×4 mm frames showing differences correlated with stimuli. Right: Demonstration of lack of invariance of AM patterns with respect to stimuli, showing that AM patterns are not representations of stimuli; they are operators containing activated memory about stimuli (center frames), which is subject to continual updating with new experience (right frames). The vertical differences reflect short-term memory changes upon the formation of an assembly. The horizontal differences reflect long-term memory changes in consolidation. From ref. [8]

ECoG spatial patterns of amplitude modulation and phase modulation

Bulbar sensation of a microscopic sensory input is expressed in high pulse frequencies of axons in the sparse network of an assembly. Perception of the input is expressed in a spatial pattern of ECoG, specifically the spatial patterns of amplitude modulation (AM) accompanied by phase modulation (PM) of the gamma carrier frequency in the band pass filtered ECoG. All neurons in the olfactory bulb contribute to the AM pattern (Fig. 2). It is mesoscopic, because it is continuous over the entire bulb, and in every local neighborhood it is the sum of dendritic current from 10^4 to 10^5 neurons. The carrier wave of the AM pattern has the same waveform and mean frequency over the entire bulb, so the AM and PM patterns are both embedded in and revealed by the band pass filtered ECoG in each stepped window. The realization of microscopic dynamical properties in AM and PM mesoscopic ordered patterns is the theoretical challenge to which the many-body model answers by using the mechanism of spontaneous breakdown of symmetry (see Section 5).

The 64 ECoG signals recorded from an 8×8 array forming a 4×4 mm window onto the bulb yield 64 amplitude values in a 64×1 feature vector, $A_{x,y}(t)$, at each time step. The tip of the vector inscribes a trajectory in 64-space. Small steps of the trajectory reveal the maintenance of a stable pattern. On repeated trials with the same stimulus the trajectory returns to the same region of 64-space. The center of gravity and surrounding standard deviation (SD) define the AM pattern for a learned stimulus and its assembly. Different stimuli have different assemblies and patterns, so that AM patterns of ECoG are classifiable with respect to learned stimuli. Unlike the microscopic sensory information, the mesoscopic classificatory information is non-local; no channel has any more or less value in classification than any other. However, the AM

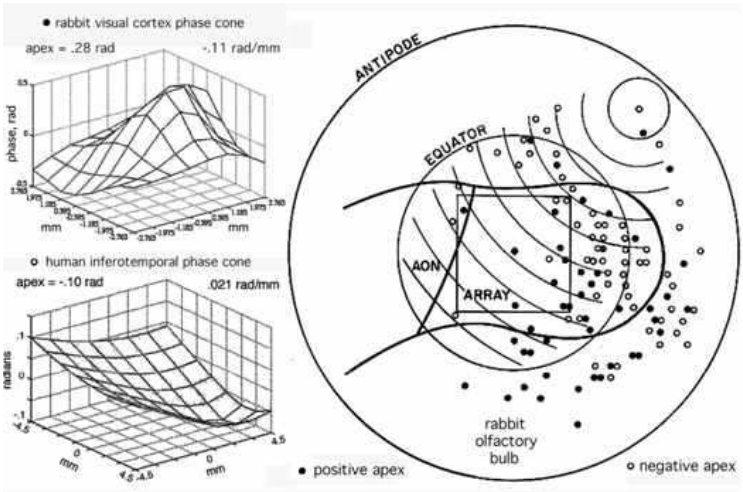

Figure 3. The silhouette shows the outline of the olfactory bulb, on which is superimposed a 4×4 mm rectangle giving the position of the surgically placed 8×8 electrode array. The two circles specify the flattened surface of the spherical bulb. The solid and open dots show the locations of conic apices. The arcs show the isophase contours of one phase cone at 0.1 rad intervals. The insets at left give examples of phase cones respectively from rabbit and human. [Adapted from ref. [9]]

patterns lack invariance with respect to invariant stimuli; instead they vary with the context and history of the individual subject. As expected for an associative memory, the AM patterns change on assimilation to any new AM pattern formation. They express the contextual meaning of the stimuli as they emerge from the memory store, which structurally is stored in the modified synaptic gains (k_{ee} in Fig. 1). These features are specifically predicted by the dissipative many-body model (see Section 5). The contextual nature of the meaning and its emergence as a product of the nonlinear relation between the brain, its *experience* (memory), and its surroundings can be traced back to formal (mathematical) aspects of the dissipative model.

Phase cones

The PM pattern, $\phi_{x,y}(t)$, of the 8×8 phase values that accompany the AM pattern of the carrier wave at its relatively fixed frequency has the shape of a cone in the cortical surface coordinates (Fig. 3). The location and sign (lag '$\circ$' or lead '$\bullet$') of the cone vary randomly from each AM pattern to the next but are fixed within AM patterns. The phase gradient in rad/mm of the cone varies randomly inversely with the carrier frequency in rad/sec; the mean phase velocity from the ratio in m/sec is invariant and equals the mean conduction velocity of cortical axons running parallel to the surface [9]. Maps of the phase cones on the cortical surface show that they last 3 to 5 cycles of the carrier oscillation. The phase cone, $\phi_{x,y}(t)$, helps to determine the location, diameter, starting time, and duration of each event containing an AM pattern, but it has no classificatory value with respect to stimuli.

Display of the filtered ECoG amplitude by frames at twice the digitizing rate in a movie (Fig. 4) shows two overlapping AM patterns with different locations, carrier frequencies, and PM patterns. One focus oscillates with the repeated expansion of alternating positive and negative peaks (+o-o+). The other focus oscillates with alternating positive and negative peaks (PNP) rotating counterclockwise about a fixed point which corresponds to the downward apex of a phase cone with maximal lag (implosion). Hence the conic phase gradients are time-dependent (Fig. 5) with six observed types of spatial PM patterns: repetitive expansion (explosion), contraction

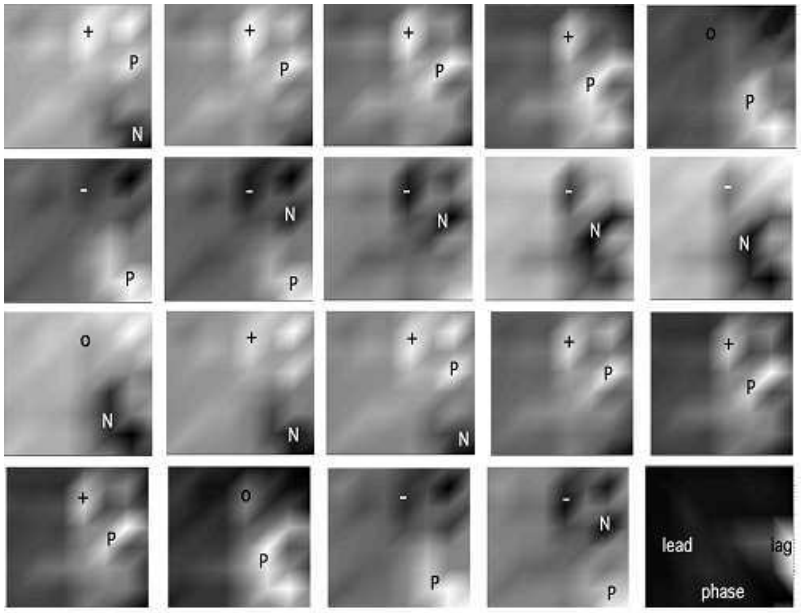

Figure 4. Frames from a 5.6×5.6 mm 8×8 electrode array were shown in time steps of 4 ms of ECoG filtered in a pass band $20 - 25$ Hz. A small focus $(+ \circ - \circ +)$ oscillated in place with cycle duration near 48 ms, the other focus rotated counterclockwise with cycle duration near 46 ms. Each pattern persisted for several cycles, then terminated. Four to six independent phase-locked ECoG patterns commonly overlapped, giving the appearance of a pan of boiling water.

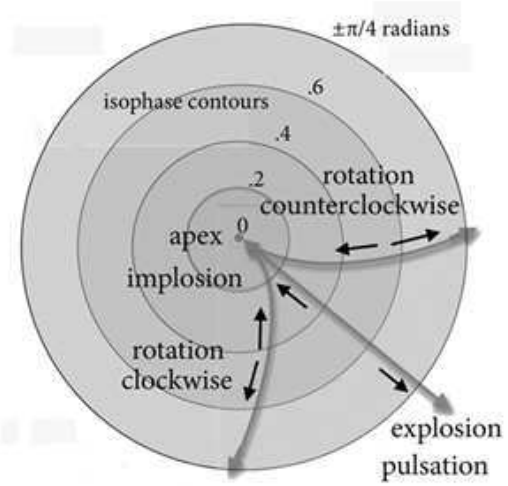

Figure 5. The conic phase gradients were either inward (implosion) or outward (explosion); they rotated clockwise or counterclockwise or pulsed without rotation.

(implosion), with or without clockwise rotation, or counterclockwise rotation. The dissipative model accounts for these observed types of spatial PM patterns and the behavior of the phase gradients.

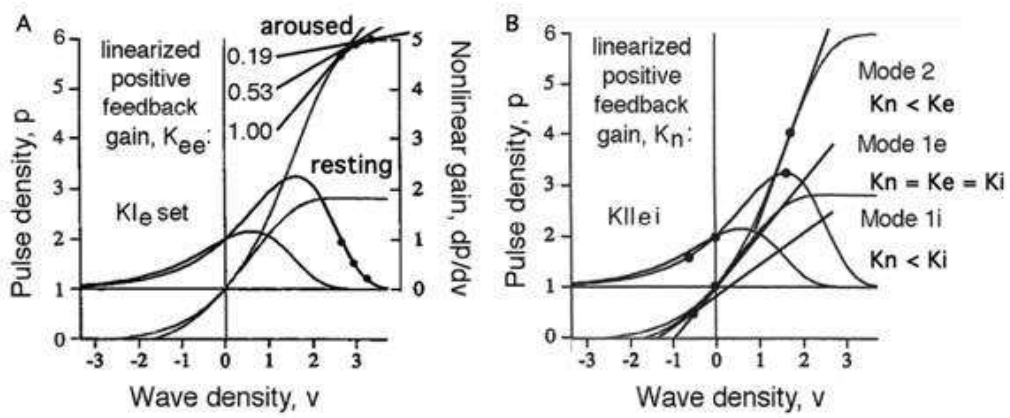

Figure 6. The linearized gain is calculated by fitting a tangent to the operating point of the nonlinear gain, dp/dv. The steady states at unity gain differ for positive (A) vs. negative (B) feedback. The asymmetric function $G(v)$ provides input-dependent gain (B, Mode 2) that is crucial for induction of phase transitions. Maximal gain, Q_m, increases with arousal (here from $Q_m = 2$ at rest to $Q_m = 5$). From [10].

3. Spontaneous background activity and oscillatory carrier waves

Cortical dynamics is expressed in networks of populations, each population representing a node. The dynamics of the network of nodes is described by a set of nonlinear integro-differential equations. Experiments have demonstrated that each population has a small-signal, near-linear domain. Thus, the equation for each neural population can be decomposed into linear time- and distance-dependent functions, $F(t)$, $H(x, y)$, describing spatial and temporal integration by dendrites, and the static nonlinear function, $G(v)$, describing the conversion (Fig. 6) of wave density v to pulse density p at trigger zones:

$$p(x, y, t) = F(t)H(x, y)G(v) \ . \tag{1}$$

The conversion of pulse density to wave density at synapses is:

$$v(x, y, t) = k_{ij}p(x, y, t) \ , \tag{2}$$

where the "gain" k_{ij} is a coefficient of proportionality from the j-th population to the i-th population. The dendritic conversion in self-regulated activity of neuronal feedback is kept within a near-linear range by the limitation in range at the trigger zone. This restriction is violated by external stimulation, such as by application of electric shocks. See Ref. [4] for details on the description of neural activity by means of ordinary linear differential equations. Here we observe that the parameters for learning and habituation are the gains k_{ee} and k_{ei} at synapses selected by input and by reinforcement under limbic control.

The operating point in the steady state is at unity gain, $dp/dv = 1$, when input and output amplitudes are equal (see Fig. 6). Demonstration of stability properties is by varying the input intensity and measuring the amplitude and rates of rise and decay of impulse responses (Fig. 7). The sequence of solutions is plotted as root loci in the complex plane. Both the amplitude and the decay rate extrapolate linearly to threshold at zero. This implies the existence of a pole at the origin of the complex plane and shows that the background activity is self-regulated by the refractory periods in every local area of cortex. The hypothesis is proposed that the pole represents a point attractor that maintains the spontaneous background activity at a set point, which is regulated by multifactorial limbic control. The control parameter Q_m is expressed by the value of the asymptotic maximum.

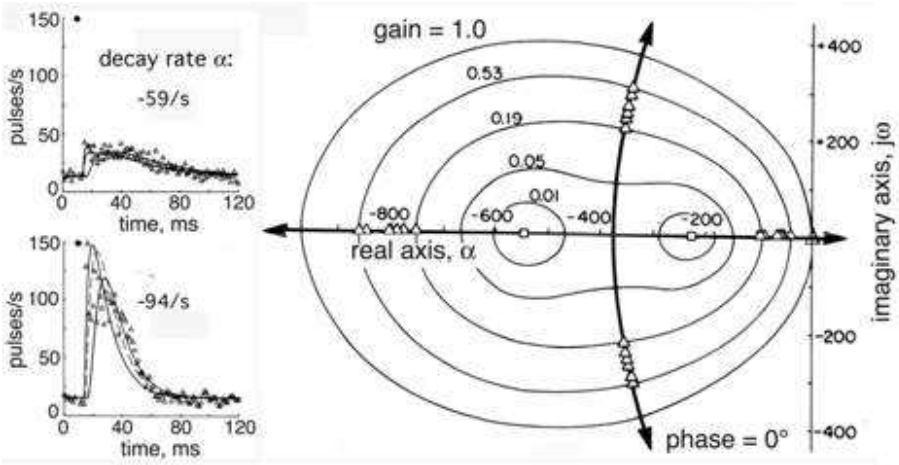

Figure 7. Left: Impulse responses of a periglomerular cell on excitation of the primary olfactory nerve at 6 intensities. Data (△) in averaged post-stimulus time histograms were fitted with solutions to a matrix of six 1st order ODE. Right: Root loci (dark lines) of the changes in poles as a function of gain (elliptical contours), k_p. At zero gain the poles (△) lie at the open loop values (□), rise rate $= -530/s$, decay rate $= -230/s$. The left-right arrows indicate the direction of change in the real rate constants as gain contours (ellipses) increase to infinity. The up-down arrows show the direction of approach of the complex conjugate roots to zeroes in the right half of the complex plane (not shown). From Fig. 5.10 p. 289, Fig. 5.13 p. 292 in [11].

The oscillatory carrier wave (inset in Fig. 2) in the gamma range $(20 - 80\ Hz)$ is generated by negative feedback interaction of the excitatory neurons ('△') with inhibitory neurons ('∘' in Fig. 1). Each neuron interacts with 10^4 other neurons, so the ECoG is mesoscopic. Modeling shows that the synapses that undergo modification in learning are not those in the negative feedback loop, k_{ei} and k_{ie}; the modified synapses are between the co-excited excitatory neurons, k_{ee}. A 20% increase in synaptic gain is shown by simulation to give 50-fold increase in the output power (Fig. 8). Activation by unwanted input is reduced by habituation, so that a 25% decrease in synaptic gain decreases power by as much as 10^{-3} attenuation [11]. The simulation of these mesoscopic properties show that the Hebbian assembly is a powerful signal amplifier and noise attenuator, and that these operations are enhanced by Q_m in arousal (Fig. 6), but it does not explain how the neural populations undergo phase transitions by which the AM pattern corresponding to a selected assembly is actualized.

The analysis of the root loci properties indicate that a limit cycle attractor exists in cortical dynamics at or near the frequency of the complex pole pair (△). If the operating point were to shift to the right across the imaginary axis with increasing ratio of amplitude to background noise, the root loci predict that the amplitude would continue to increase without limit, as the operating point approached the limit cycle attractor, at which a singularity would occur. This prediction cannot be tested experimentally with linear analysis, because the impulse responses must converge for observation. Nonlinear analysis indicates that this trajectory does occur and is responsible for the phase transition owing to the spontaneous fluctuations. It has now become apparent that the fluctuations can be attributed to fluctuations in the background activity, because the driving input is constant, and no changes in sensitivity occur with learning. The proposed mechanism is the beats in Rayleigh noise, which are power minima in band pass filtered noise that alternate with power maxima.

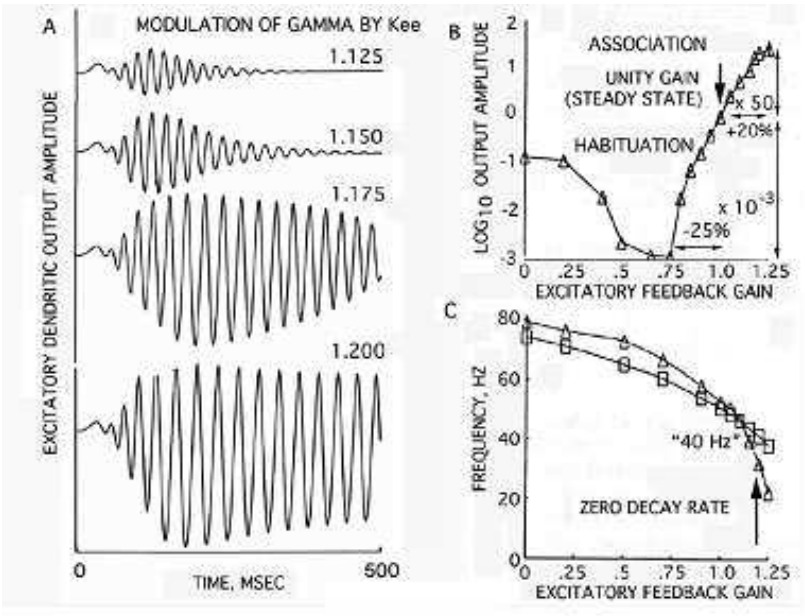

Figure 8. Negative feedback between excitatory and inhibitory neurons sustains oscillation in the gamma range ($20 - 80$ Hz). An assembly forms by selective strengthening of synaptic connections (A). Increased excitatory feedback gain, k_{ee}, in reinforcement learning increases the power (B) and decreases the frequency (B) of the oscillations selectively on reception of the learned input. Habituation decreases the sensitivity of the olfactory system to unreinforced stimuli [10].

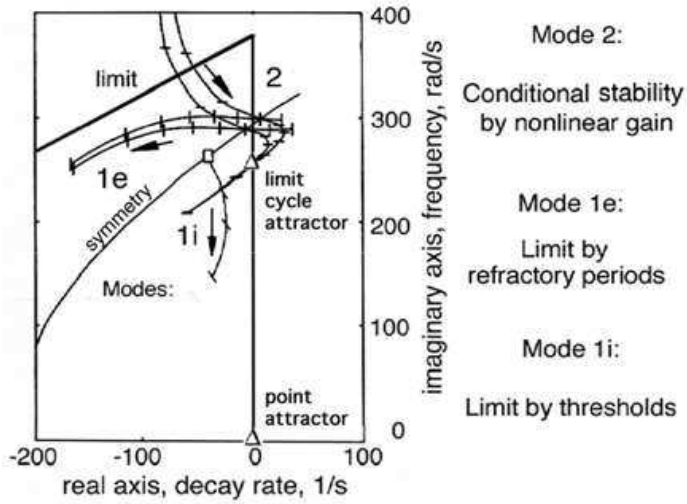

Figure 9. Root loci (solution sets for linearized gains, $k_{ee},\ k_{ei},\ k_{ie},\ k_{ii}$) are shown in the upper half of the complex plane (one of a pair of complex conjugate roots) for three families of root loci. The control parameter for movement along trajectories is the output amplitude. Arrows show direction of pole movement with increasing ratio of response amplitude to background activity. The stable point attractor at the origin governs the level of the background activity. The limit cycle attractor manifests a singularity, because if the operating point is shifted into the right half of the complex plane, the increase in amplitude carries it inexorably to the attractor. Crossing the imaginary axis in phase transition requires that four conditions be met: formation of an assembly (Fig. 1), arousal (Fig. 6), input that selectively activates the assembly and spontaneous suppression of the order parameter, $\mathbf{A}^2(t)$, in a null spike (Fig. 10) from Rayleigh noise. Adapted from Fig. 6.30, p. 388 in [11].

4. Null spikes, phase transitions and scale-free dynamics in perception

In piecewise linear analysis, the operating point moves along a trajectory in Mode 2 across the imaginary axis into the right half of the complex plane by reducing the background activity. The sudden decrease in the amplitude of the band pass filtered ECoG (Fig. 10, A, C) manifests a decrease in the order parameter, $\mathbf{A}^2(t)$. The crossing of the operating point into the right half of the complex plane is revealed by a beat that precedes a phase transition.

The event repeats as down spikes in $\log_{10}$ power (D), the deepest of which are labeled null spikes. The analytic phase (B) from the Hilbert transform [12] at these points is indeterminate, as reflected in wide deviations of the analytic frequency (D) and the increased spatial standard deviation of the analytic phase, $SD_X(t)$ [13].

The neural mechanism of down spikes in ECoG stems from that of the background activity in mutual excitation. The microscopic action potentials that carry the self-regulated activity are modeled as independent Poisson processes collectively generating white noise, which is easily simulated by time series of random numbers. The cumulative sum simulates the mesoscopic ECoG background activity that conforms to brown noise ($1/f^2$) [14, 15] and more specifically to black noise ($1/f^\alpha,\ 2 < \alpha < 4$) [16, 17]. These time series have continuous power spectral densities (PSD). Inhibition does not change the power-law PSD in the rest state of symmetry where $k_n = k_{ee} = k_{ei}$ (symmetry in Fig. 9). The scale-free cortical dynamics [18] gives the power-law PSD, so that band pass filtering the simulated and real ECoG gives beats (Rayleigh noise) of alternating maxima and minima (Fig. 10, A) for every pass band in the relevant spectral range ($1 - 100$ Hz). The beat frequencies are distributed; the modal beat frequency for both simulated noise and ECoG is proportional to the bandwidth by a factor of 0.641 [19] at every center frequency [20].

These coincident spikes serve as approximate indicators of temporal locations of phase transition. The precise location is indicated by a temporal discontinuity in the analytic phase [21], at which the analytic frequency jumps to a new value in what appears as *phase slip* [22] immediately preceding the appearance and stabilization of new AM patterns with phase cones [23].

Proof that the null spikes are intrinsic to the neural mechanisms governing microscopic and mesoscopic background activity is by replicating the wave forms of the analytic power and frequency of the EEG (Fig. 10, A); the power-law distributions of power spectral density (PSD) of the EEG at rest and in sleep (Fig. 11, A) [17]; the distributions of $\log_{10}$ analytic power of downward spikes (C, D) [15], and the distributions of the durations of frames between null spikes (B) [20].

These experimental data provide the evidence needed to construct a dissipative dynamic hypothesis of perception. The turbulence in the ECoG at the cortical surface illustrated in Fig. 4 holds in every pass band in the clinical range, conforming to the scale-free dynamics predicted from the power-law PSD of the resting ECoG (Fig. 11, A) and other variables [12]. The existence of a pole at the origin of the complex plane (Fig. 7) shows that cortex homeostatically holds its operating point at or very near a state of criticality, which can justifiably be called self-organized, because it is kept at a homeostatically controlled set point by randomly distributed, abortive phase transitions that are manifested in phase cones (Fig. 3) having power-law distributions of durations and diameters. Few among the phase cones have durations that exceed those expected for noise [Fig. A1.08 in [23]; Section 3.4 and Fig. 2.06, E in [21]], and these few fall into the Rice distribution with longer durations than inter-spike intervals in the Rayleigh distribution [20]. That is significant, because these frames accompany classifiable AM patterns (Fig. 2) that last long enough to transmit 3 to 5 cycles of the carrier frequency [25], and they also have the long correlation distances needed to span vast areas of primary sensory cortices. These attributes of size and persistence make them prime candidates for the neural correlates of retrieved memories.

Null spikes set the system in the symmetric (zero order parameter) ground state so that

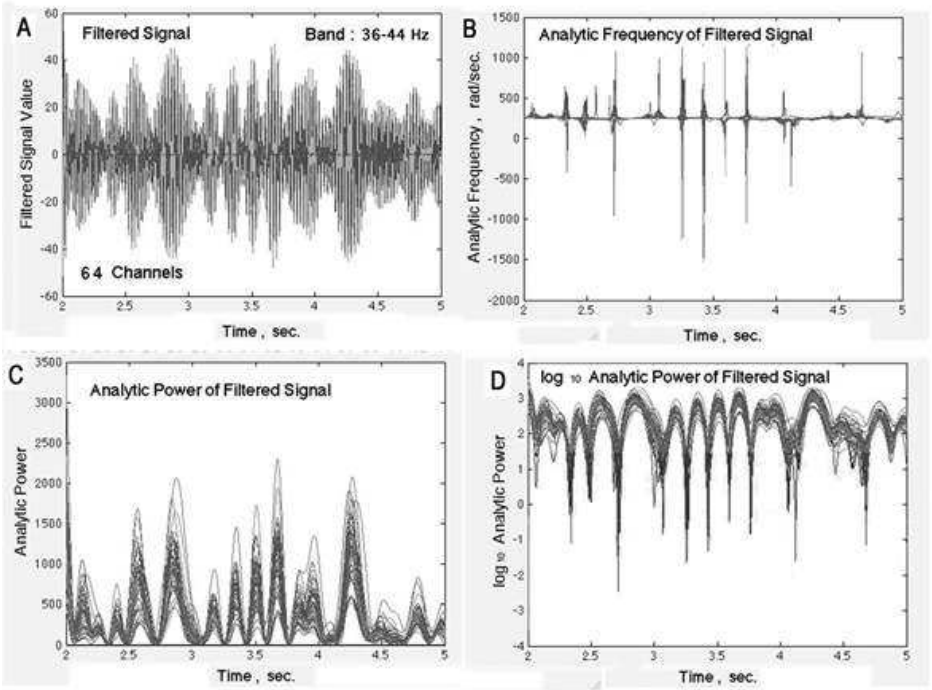

Figure 10. Null spikes are observed by band pass filtering the EEG (A), applying the Hilbert transform [24] to get the analytic power (B), and taking the logarithm (C). On each channel the downward spikes coincide with spikes in analytic frequency (D) reflecting increased analytic phase variance. The flat segment between spikes reflects the stability of the carrier frequency of AM patterns. The spikes form clusters in time but are not precisely synchronized. One or more of these null spikes coincides with phase transitions leading to emergence of AM patterns. The modal repetition rate of the null spikes in Hz is predicted to be 0.641 times the pass band width in Hz (p. 90, Equation 3.8-15 in ref. [19]).

spontaneous symmetry breaking (Mode 2) may then occur. When that happens, the sensory input that activates a Hebbian assembly already formed by learning introduces into the broken symmetry a powerful narrow-band gamma burst (Fig. 8) that is facilitated by the increased synaptic gain, k_{ee}, with learning (Fig. 1), the increased control parameter, Q_m, with arousal, and the asymmetric gain around the operating point (Fig. 6).

5. Dissipative many-body neurodynamics

In the previous Sections we have seen that the mesoscopic neural activity of neocortex appears in laboratory observations to consist of the dynamical formation of spatially extended domains in which widespread cooperation supports brief epochs of patterned oscillations. In 1967 Umezawa and Ricciardi [26, 27, 28] proposed to describe the collective neural activity which manifests in the formation of spatially extended domains by using the mechanism of spontaneous breakdown of symmetry in quantum field theory (QFT). By resorting to preceding studies on the physics of living matter [29, 30, 31] and to the QFT formalism for dissipative systems [32], the extension to the dissipative dynamics of the Umezawa and Ricciardi many-body model has been worked out [33, 3] and the comparison of the predictions of the dissipative quantum model of brain with the laboratory observations has been pursued [34, 6, 35].

It appears that the dissipative model predicts the experimentally observed coexistence of physically distinct amplitude modulated (AM) and phase modulated (PM) patterns correlated with categories of conditioned stimuli and the remarkably rapid onset of AM patterns into irreversible sequences that resemble cinematographic frames [34, 6]. The dissipative model also

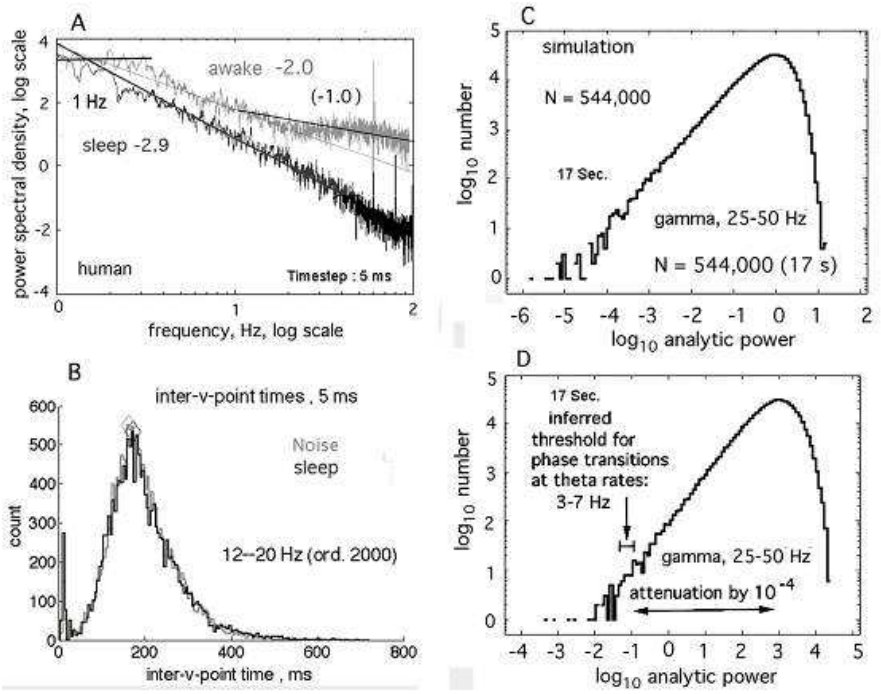

Figure 11. Evidence is summarized showing that the mesoscopic background activity conforms to scale-free, low-dimensional noise [18]. Engagement of the brain in perception and other goal-directed behaviors is accompanied by departures from randomness upon the emergence of order (A), as shown by comparing PSD in sleep, which conforms to black noise, vs. PSD in an aroused state showing excess power in the theta ($3-7$ Hz) and gamma ($25-100$ Hz) ranges. B. The distributions of time intervals between null spikes of brown noise and sleep ECoG are superimposed. C,D. The distributions are compared of $\log_{10}$ analytic power from noise and ECoG. Hypothetically the threshold for triggering a phase transition is 10^{-4} down from modal analytic power. From [15, 17]

accounts for the formation of phase cones and vortices in the transition from one AM pattern to another one [6].

The collective behavior of an ensemble of a large number of elementary components is the object of study of Statistical Mechanics. In the case of neural components, Hopfield [36] asked whether stability of memory and other macroscopic properties of neural nets are also derivable as collective phenomena and emergent properties. Classical Statistical Mechanics provides very powerful tools in answering Hopfield's question [37, 38]. However, at a classical level analysis, the electric field of the extracellular dendritic current and the magnetic fields inside the dendritic shafts appear to be much too weak and the chemical diffusion appears to be much too slow to be able to fully account for the cortical collective activity observed in laboratory [14, 6]. Molecular (neuro-)biology provides crucial tools in the discovery of many mechanisms and chemical functions in brains and living matter in general. The question is now how to put together all these data so to derive the complex behavior of the whole system. In this connection, Schrödinger has introduced the important distinction between the "two ways of producing orderliness" (p.80 of ref. [39]), namely, ordering generated by the "statistical mechanisms" and ordering generated by "dynamical" interactions among the atoms and the molecules, which, as it is well known, are *necessarily* quantum interactions.

The functional stability in living systems is characterized by time ordering of pathways of biochemical reactions sequentially interlocked. Common laboratory experience is that even the simplest chemical reaction pathway, once embedded in a random chemical environment, soon

collapses. Chemical efficiency and functional stability to the degree observed in living matter, i.e. not as "regularity only in the average" [39], appears to be out of reach of any probabilistic approach *solely* based on microscopic random kinematics. Thus, it is still a *matter of belief* that out of a purely random kinematics there may arise with high probability a unique, time ordered sequence of chemical reactions as the one required by the macroscopic history of the system. It is a fact that, although highly sophisticated probabilistic methods have been developed, there is no available computation or even abstract proof which shows how to obtain the characteristic chemical efficiency and stability of living matter by resorting uniquely to statistical concepts. In Schrödinger's words: "it needs no poetical imagination but only clear and sober scientific reflection to recognize that we are here obviously faced with events whose regular and lawful unfolding is guided by a "mechanism" entirely different from the "probability mechanism" of physics" (p.79 of ref. [39]). Classical statistical mechanics and short range forces of molecular biology, *although necessary*, do not seem to be completely adequate tools. Therefore, it appears to be necessary to supplement them with a further step so to include underlying quantum *dynamical* features. Moreover, one more motivation to follow the research path pioneered by Schrödinger is in the fact that there is no conventional neural network offered by neuroscientists or neuroengineers that can adequately model or simulate the neurophysiological data on the brain activity which are today available [35]. In another approach, random graph theory modified as neuropercolation theory shows promise in complementing the use of ordinary and partial differential equations [18].

Such a conceptual frame and the experimental observations motivated the formulation of the many-body model for the brain and its subsequent extension to the dissipative dynamics.

The model central feature rests on the fact that patterns of correlated elements (ordered patterns) are described in QFT by the mechanism of spontaneous breakdown of symmetry (SBS). The observable specifying the degree of ordering of the system vacuum is called the order parameter and acts as a macroscopic variable. It is related with the density of coherently condensed Nambu-Goldstone (NG) bosons in the system ground state and may be considered to be the *code* specifying the system macroscopically observable ordered state, namely its physical phase, among many possible degenerate ground states (vacua). In the quantum model of the brain the code of the ground state specifies its memory content: the memory recording process is depicted by the NG boson condensation in the brain ground state. The external informational input acts as the trigger of the symmetry breakdown out of which the NG bosons and their condensation are generated. The recall of the recorded information occurs under the input of a stimulus "similar" to the one responsible for the memory recording [26] (see also ref. [40]).

We stress that the external stimulus only acts as a trigger inducing the SBS, the specific ordered pattern being generated by the "internal" brain dynamics, which, except for the breakdown of the symmetry, is not conditioned by the external stimulus (*spontaneous* breakdown of the symmetry). This model feature is perfectly consistent with laboratory observations mentioned in Section 2; it accounts for the observed lack of invariance of AM patterns with invariant stimuli [34, 41, 42].

A different regime is, in contrast, obtained when symmetry is *explicitly* broken, as, for example, under the effect of an electric shock, by which the cortex dynamics is enslaved with consequent response by the so-called evoked or *event-related potential* (ERP). The explicit breakdown in cortical dynamics is observed by resort to stimulus-locked averaging across multiple presentations in order to remove or attenuate the background activity, so as to demonstrate that the location, intensity and detailed configuration of the ERP is predominantly determined by the stimulus.

The symmetry which gets broken is the rotational symmetry of the electrical dipoles of the water molecules [43, 44, 45] and the NG modes are the vibrational dipole wave quanta (DWQ) [29, 30, 31]. The whole brain dynamics is indeed embedded in a matrix of molecules carrying

the quantum degree of freedom associated to the electric dipole oscillatory motion. The well known electrical properties of cell membranes and the experimental observations [46, 47] of slow fluctuations in neuronal membrane polarization (the so-called up and down states) corresponding to that of spontaneous fluctuations in the fMRI signal confirm that one cannot ignore the electrical dipole oscillatory matrix in which the neuronal electrophysical and electrochemical activity is embedded [48]. Thus, the electric dipole vibrational field dynamics at basic molecular level cannot be without effects on the rich electrochemical and biochemical activity observed at the neural classical level.

We stress that *no ambiguity should be born on the point that neurons and other brain cells are by no means considered quantum objects in the dissipative many-body model.* The dissipative many-body model differs in a substantial way from brain models formulated in the Quantum Mechanics frame, such those discussed in refs. [49, 50, 51]. In contrast with such last models, *the neurons, the glia cells and other brain cells are classical systems in the dissipative many-body model.*

Let us very briefly summarize some formal aspects of the dissipative model. For details see refs. [33, 3].

The procedure of the canonical quantization of a dissipative system requires the "doubling" of the degrees of freedom of the system [32] in order to ensures that the flow of the energy exchanged between the system and the environment is balanced.

Let A_k and $\tilde{A}_k$ denote the annihilation operators for the DWQ mode and its "doubled mode", respectively. k denotes the momentum and other specifications of the A operators ($A_k^\dagger$ and $\tilde{A}_k^\dagger$ denote the creation operators). Let $\mathcal{N}$ be the *code* imprinted in the vacuum at the initial time $t_0 = 0$ by the external input and representing the *memory record* of the input. The code $\mathcal{N}$ is the set of the numbers $\mathcal{N}_{A_k}$ of modes A_k, for any k, condensate in the vacuum state denoted by $|0>_{\mathcal{N}}$, which thus represents the memory state at $t_0 = 0$ [33, 52]. $\mathcal{N}_{A_k}(t)$ is given, at each t, by:

$$\mathcal{N}_{A_k}(t) \equiv {}_{\mathcal{N}} < 0(t)|A_k^\dagger A_k|0(t) >_{\mathcal{N}} = \sinh^2(\Gamma_k t - \theta_k) \quad , \tag{3}$$

and similarly for the modes $\tilde{A}_k$. Γ_k is the damping constant (related to the memory life-time of the mode k) and θ_k fixes the code value at $t_0 = 0$. The state $|0(t) >_{\mathcal{N}} \equiv |0(\theta, t) >$ is the time-evolved of the state $|0>_{\mathcal{N}}$ at $t_0 = 0$ and is given by:

$$|0(t)\rangle = \prod_\kappa \frac{1}{\cosh(\Gamma_\kappa t - \theta_k)} \exp\left(\tanh(\Gamma_\kappa t - \theta_k) A_\kappa^\dagger \tilde{A}_\kappa^\dagger\right)|0\rangle \ . \tag{4}$$

$|0>_{\mathcal{N}}$ and $|0(t)>_{\mathcal{N}}$ are normalized to 1 and in the infinite volume limit we have

$$_{\mathcal{N}} < 0(t)|0 >_{\mathcal{N}'} \underset{V\to\infty}{\longrightarrow} 0 \quad \forall\, t \neq t_0, \quad \forall\, \mathcal{N}\ , \mathcal{N}'\ , \tag{5}$$

$$_{\mathcal{N}} < 0(t)|0(t') >_{\mathcal{N}'} \underset{V\to\infty}{\longrightarrow} 0, \quad \forall\, t\,, t' \text{ with } \quad t \neq t'\ ,\ \forall\, \mathcal{N},\ \mathcal{N}'\ , \tag{6}$$

with $|0(t) >_{\mathcal{N}'} \equiv |0(\theta', t) >$. Eqs. (5) and (6) also hold for $\mathcal{N} \neq \mathcal{N}'$, $t = t_0$ and $t = t'$, respectively. Eqs. (5) and (6) show that in the infinite volume limit the vacua of the same code $\mathcal{N}$ at different times t and t', for any t and t', and, similarly, at equal times, but different $\mathcal{N}$'s, are orthogonal states. The corresponding Hilbert spaces are unitarily inequivalent spaces. The number $\left(\mathcal{N}_{A_k} - \mathcal{N}_{\tilde{A}_k}\right)$ is a constant of motion for any k and θ. The physical meaning of the $\tilde{A}$ system is the one of the sink where the energy dissipated by the A system flows. The $\tilde{A}$ modes describe the thermal bath or the environment modes.

The balance of energy flow between the system and the environment is ensured by the requirement $\mathcal{N}_{A_k} - \mathcal{N}_{\tilde{A}_k} = 0$, for any k. Such a requirement, however, does not uniquely fix the code $\mathcal{N} \equiv \{\mathcal{N}_{A_k}, \text{ for any } k\}$. Also $|0>_{\mathcal{N}'}$ with $\mathcal{N}' \equiv \{\mathcal{N}'_{A_k}; \mathcal{N}'_{A_k} - \mathcal{N}'_{\tilde{A}_k} = 0, \text{ for any } k\}$ ensures

the energy flow balance. Thus, also $|0>_{\mathcal{N}'}$ is an available memory state: it corresponds, however, to a different code number ($i.e. \mathcal{N}'$) and therefore to a different information than the one of code $\mathcal{N}$. In the infinite volume limit $\{|0>_{\mathcal{N}}\}$ and $\{|0>_{\mathcal{N}'}\}$ are representations of the canonical commutation relations each other unitarily inequivalent for different codes $\mathcal{N} \neq \mathcal{N}'$. Thus, infinitely many memory (vacuum) states, each one of them corresponding to a different code $\mathcal{N}$, may exist: a huge number of sequentially recorded inputs may *coexist* without destructive interference since infinitely many vacua $|0>_{\mathcal{N}}$, for all $\mathcal{N}$, are *independently* accessible in the sequential recording process.

In conclusion, the "brain (ground) state" is represented as the collection (or the superposition) of the full set of states $|0>_{\mathcal{N}}$, for all $\mathcal{N}$. The brain is thus described as a complex system with a huge number of macroscopic states (the memory states).

The degree of the coupling of the system A with the system $\tilde{A}$ can be parameterized by an index, say n, in such a way that in the limit of $n \to \infty$ the possibilities of the system A to couple to $\tilde{A}$ (the environment) are "saturated": the system A then gets *fully* coupled to $\tilde{A}$. It can be shown [52] that a higher or lower *degree of openness* (measured by n) to the external world may produce a better or worse ability in setting up neuronal correlates, respectively (different under different circumstances, and so on, e.g. during the sleep or the awake states, the childhood or the older ages). The functional or effective connectivity (here we do not consider the structural or anatomical one) is highly dynamic in the dissipative model. Once these functional connections are formed, they are not necessarily fixed. On the contrary, they may quickly change and new configurations of connections may be formed extending over a domain including a larger or a smaller number of neurons. The finite size of the correlated domain implies a non-zero effective mass of the DWQs. These propagate through the domain with a greater inertia than in the case of large (infinite) volume where they are (quasi-)massless. The domain correlations are then established with a certain time-delay, which contributes to the delay observed in the recruitment of neurons in a correlated assembly under the action of an external stimulus.

Free energy, phase transitions and attractor landscape

One can show [33] that the minimization of the free energy, $d\mathcal{F}_A = dE_A - \frac{1}{\beta} d\mathcal{S}_A = 0$, is ensured and the change in time $d\mathcal{N}_A$ of particles condensed in the vacuum turns into heat dissipation $dQ = \frac{1}{\beta} dS$.

In the infinite volume limit Eqs. (5) and (6) also hold true for $\mathcal{N} = \mathcal{N}'$. Time evolution of the state $|0\rangle_{\mathcal{N}}$ is thus represented as the (continual) transition through the representations $\{|0(t)\rangle_{\mathcal{N}}, \ \forall \mathcal{N} \ , \ \forall t\}$, namely by the "trajectory" through the "points" $\{|0(t)\rangle_{\mathcal{N}}, \ \forall \mathcal{N} \ , \ \forall t\}$ in the space of the representations (each one minimizing the free energy functional). The trajectory initial condition at $t_0 = 0$ is specified by the $\mathcal{N}$-set. It can be shown [55, 56, 57] that: *a)* these trajectories are classical trajectories and *b)* they are chaotic trajectories. This means that the trajectories are bounded and each trajectory does not intersect itself; there are no intersections between trajectories specified by different initial conditions and trajectories of different initial conditions are diverging trajectories. The property that trajectories specified by different initial conditions ($\mathcal{N} \neq \mathcal{N}'$) never cross each other implies that no *confusion* (interference) arises among the codes of different neuronal correlates, even as time evolves. In realistic situations of finite volume, states with different codes may have non–zero overlap (the inner products Eqs. (5) and (6) are not zero). In such a case, at a "crossing" point between two, or more than two, trajectories, there can be "ambiguities" in the sense that one can switch from one of these trajectories to another one which there crosses. This may be felt indeed as an *association* of memories.

For a very small difference $\delta\theta_k \equiv \theta_k - \theta'_k$ in the initial conditions of the two initial states, the difference between originally even slightly different $\mathcal{N}_{A_k}$'s can be shown to grow as time evolves.

For large enough t, the modulus of the difference $\Delta\mathcal{N}_{A_k}(t)$ and its time derivative diverge as $\exp(2\Gamma_k t)$, for all k's. This may account for the high perceptive resolution in the recognition of the perceptual inputs. Moreover, the difference between k–*components* of the codes $\mathcal{N}$ and $\mathcal{N}'$ may become zero at a given time $t_k = \frac{\theta_k}{\Gamma_k}$. However, the difference between the codes $\mathcal{N}$ and $\mathcal{N}'$ does not necessarily become zero. The codes are different even if a finite number of their components are equal since they are made up by a large number of $\mathcal{N}_{A_k}(\theta, t)$ components (infinite in the continuum limit). Suppose that, for $\delta\theta_k \equiv \theta_k - \theta'_k$ very small, the time interval $\Delta t = \tau_{max} - \tau_{min}$, with τ_{min} and τ_{max} the minimum and the maximum, respectively, of $t_k = \frac{\theta_k}{\Gamma_k}$, for *all* k's, be very small. Then the codes are recognized to be *almost* equal in such a Δt, which then expresses the recognition (or recall) process time. This shows how it is possible that "slightly different" $\mathcal{N}_{A_k}$–patterns (or codes) are recognized to be the *same code* even if corresponding to slightly different inputs. We also remark that the vacua $\{|0(t)\rangle_{\mathcal{N}},\ \forall\mathcal{N}\ ,\ \forall t\}$, through which trajectories go, behave as nonlinear dynamical "attractors" since they are the system ground states (for each $\mathcal{N}$ at each t). Their manifold, which constitutes the space of the brain states, may be thus thought as the attractor landscape for the (nonlinear) brain dynamics. The fact that the dissipative quantum model brings to the classicality of the trajectories through such a space of brain states is one of the model major merits [6, 35].

In the engagement of the brain with the environment in the action-perception cycle, the existing attractor landscape provides the "accumulated experience", or the "knowledge", or the"context" in which the new perception happens to be situated (cf. Section 2). Under the influence of the new perception the brain reaches a new "balance" in a new vacuum, which enters the attractor landscape producing its global rearrangement. The process of the formation of the *meaning* of the newly acquired information and of its "contextualization" consists in such a global updating of the attractor landscape, which, in turn, defines and imposes the conditions to the subsequent action. The whole process involving the engagement of the brain with its environment has been referred to as the "dialog" between the brain and its *Double* (the environment is formally described by the "doubled" degrees of freedom, which express at the same time the environment and the system (brain) time-reversed image, see above). Consciousness has been proposed to be rooted in such a permanent dialog between the subject and its Double [33, 3].

Null spikes, vortices and phase cones

Time–dependence of the DWQ frequency implies that higher momentum k-components of the $\mathcal{N}$-set possess longer life–times. Momentum is proportional to the inverse distance over which the mode propagates, thus modes with a shorter range of propagation (more "localized" modes) survive longer. On the contrary, modes with a longer range of propagation decay sooner. The dissipative model thus predicts the existence of condensation domains of different finite sizes with different degrees of stability [52]. They are described by the condensation function $f(x)$, which acts as a "form factor" specific for the considered domain [53, 54], and in the presence of the e.m. field $f(x)$ has to carry some topological singularity in order for the condensation process to be physically detectable. Phase transitions driven by boson condensation are always associated with some singularity (indeterminacy) in the field phase at the phase transition point[53, 54]. The dissipative model thus accounts for the observed crucial mechanism described in Section 4: the event that initiates a perceptual phase transition is an abrupt decrease, the *null spike*, in the analytic power of the background activity to near zero. The model also accounts for the observation of vortices and propagating waves of phase gradients (the phase cones) in perceptual phase transitions. These features are summarized in the following. See details in ref. [35].

By use of the Hilbert transform, the ECoG sampled wave function $\psi(x)$ in the selected

spectral pass band is represented as

$$\psi(x) = \mathbf{A}(x)e^{i\phi(x)} \ , \tag{7}$$

where $x \equiv (x, y, t)$ in the two surface dimensions of cortex (3 dimensions for the microscopic level of networks), and the analytic power $\mathbf{A}^2(x)$ and the analytic phase $\phi(x)$ are, in terms of the real and imaginary parts $a(x)$ and $b(x)$,

$$\mathbf{A}^2(x) = a^2(x) + b^2(x) \ , \tag{8}$$

$$\phi(x) = \arctan \frac{b(x)}{a(x)} \ , \tag{9}$$

respectively. During periods of high amplitude the spatial deviation of phase (SD_X) is low and the phase spatial mean tends to be constant within frames and to change suddenly between frames, indicating coherence and coordinated phase differences. $\mathbf{A}^2(x)$ forms a feature vector that serves as our order parameter (see Section 2 and Refs. [6, 34]).

The reduction in the amplitude of the spontaneous background activity induces a brief state of indeterminacy in which the power in significant pass band of the electrocorticogram (ECoG) is near zero and the phase of ECoG is undefined.

As already discussed in previous sections, the cortex can be driven across such a "phase transition" to a new AM pattern by the stimulus arriving at or just before the onset of a null spike. The observed velocity of spread of phase transition is finite, i.e. there is no "instantaneous" phase transition; it is determined by the conduction velocities of axons of intracortical neurons, not those of the input axons. Experimental evidence indicates that the neuronal correlation length would cover an entire cerebral hemisphere very quickly (practically without delay in the gamma activity), if measured at the critical transition. Between the null spikes the cortical dynamics is (nearly) stationary for $\sim 60 - 160\ ms$. This is called a frame. The transitions by which they form are shorter by an order of magnitude. The spatial phase gradient propagates as a phase cone that is imposed on the carrier wave of the wave packet in a frame by the propagation velocity of the largest axons having the highest velocity in a distribution. The location of the apex is a random variable across frames that is determined by the accidents of where the null spike is lowest and the background input is highest. The null spike has rotational energy at the geometric mean frequency of the pass band, so it is called a vortex. The vortex occupies the whole area of the phase-locked neural activity of the cortex for a point in time. One more observed feature is the random variation from each frame to the next of the slope of the spatial conic phase gradient, negative with explosion, positive with implosion. The negative gradient could be explained in conventional neurodynamics (e.g. in terms of a pacemaker), but not the positive gradient. Also, there is no explanation in the conventional framework of why both gradients, the positive and the negative one, occur.

The spontaneous breakdown of symmetry considered above leads to non-vanishing polarization density $\mathcal{P} = \rho\delta$, where ρ and δ are the charge density and the (average) dipole length, in the ground state. One then considers the (further) spontaneous breakdown of the phase symmetry and the charge density wave function $\sigma(x)$ written [30] as

$$\sigma(x) = \sqrt{\rho(x)}e^{i\theta(x)} \ , \tag{10}$$

with real $\rho(x)$ and $\theta(x)$. The "phase" $\theta(x)$ is the NG field associated with the breakdown of global phase symmetry. The boson condensation of the field $\theta(x)$ in the system ground state is formally described by the transformation

$$\theta(x) \to \theta(x) - \frac{e_0 v^2}{Z} f(x) \ . \tag{11}$$

The c-number condensation function $f(x)$ satisfies the same equation satisfied by the $\theta(x)$ field, i.e. $\partial^2 f(x) = 0$. The constant Z is the wave function renormalization constant, e_0 and v are the electron charge and the constant entering the symmetry breakdown condition $< 0|\rho(x)|0 >= v \neq 0$ [30, 58, 59]. Coherent domains of finite size are obtained by non-homogeneous boson condensation. The condensate is described by the function $f(x)$ which, as said above, acts as a "form factor" specific for the considered domain [59, 52, 53, 54]. One can show [30, 58] that mathematical consistency requires that the electromagnetic vector potential $a_\mu(x)$ has to satisfy the equation

$$(\partial^2 + m_V^2)\, a_\mu(x) \;=\; \frac{m_V^2}{e_0}\, \partial_\mu f(x)\ . \tag{12}$$

We adopt the gauge condition $\partial^\mu a_\mu(x) = 0$. Eq. (12) is the classical Maxwell equation for the massive vector potential a_μ (m_V is its mass). The classical ground state current $j_{\mu,cl}$ turns out to be

$$j_{\mu,cl}(x) \equiv \langle 0|j_\mu(x)|0\rangle \;=\; m_V^2 \left[a_\mu(x) - \frac{1}{e_0}\, \partial_\mu f(x)\right]\ , \tag{13}$$

and we have $\partial^\mu j_{\mu,cl}(x) = 0$. The term $m_V^2 a_\mu(x)$ is the well known *Meissner current*, while $\frac{m_V^2}{e_0}\partial_\mu f(x)$ is the *boson current*. The mesoscopic field and current are thus given in terms of the boson transformation function. It is also remarkable that the classical current is related with $\partial_\mu f$, i.e. with variations in the boson transformation function.

The important point is that such a condensation function $f(x)$ has to carry some topological singularity in order for the condensation process to be physically detectable. Eq. (12) implies $a_\mu(x) = \frac{1}{e_0}\partial_\mu f(x)$ for regular $f(x)$, which in turn implies zero classical field ($F_{\mu\nu} = \partial_\mu a_\nu - \partial_\nu a_\mu$) and zero classical current ($j_{\mu,cl} = 0$) since the Meissner and the boson current cancel each other. It is indeed well known [60] that the gauge field a_μ is expelled out of the ordered domain region (there it vanishes) where the order parameter is of course non-zero and $f(x)$ does not have singularities. On the contrary, the gauge field is non zero in the regions where $f(x)$ presents non-trivial topological singularities such as line singularities, e.g. on the line $r = 0$ in the core of a vortex: we have there the "normal" (disordered) state rather than the ordered one and the non-vanishing massive gauge field there propagates (the Anderson-Higgs-Kibble mechanism) [60, 61]. On the boundaries between the normal and the ordered regions the phase field gradients are non-zero. Instead they are zero in the normal region, i.e. in the vortex core. One can also show [59, 53, 54] that the phase transition from one state space to another (unitarily inequivalent) one can only be induced by a singular boson transformation function $f(x)$. We thus recognize that in the brain the null spike (the observed abrupt decrease in the order parameter and the concomitant increase in the phase field gradients in the phase transition from an AM amplitude to another one) is indeed characterized by the topological singularity of the function $f(x)$. In the case of phase symmetry summarized above, the stationary function $f(x)$ solution of our problem carries a vortex singularity and is given by

$$f(x) = \arctan\left(\frac{x_2}{x_1}\right)\ . \tag{14}$$

Eq. (14) shows that the phase is undefined on the line $r = 0$, with $r^2 = x_1^2 + x_2^2$, consistently with the observed phase indeterminacy in the process of transition between two AM pattern frames. As a result of the single-valuedness of $\sigma(x)$ the topological singularity is characterized by the winding number n: $\oint \nabla f \cdot dl = 2\pi n$, $n = 0, \pm 1, \pm 2, ...$, when the integration is performed along the closed circle $(0, 2\pi)$ (flux quantization). We also remark that clockwise rotation and counterclockwise rotation are both allowed.

As already remarked above, the dissipative model predicts that the response amplitude depends not on the input amplitude, but on the intrinsic state of the cortex, specifically the degree of reduction in the power and order of the background brown noise.

We also observe that the initial site where non-homogeneous condensation starts (the phase cone apex) is not conditioned by the incoming stimulus, but is randomly determined by the concurrence of a number of local conditions, such as where the null spike is lowest and the background input is highest, in which the cortex finds itself at the transition process time. The apex is never initiated within frames (in the broken symmetry phase or ordered region), but between frames (during phase transitions), as it is indeed predicted by the dissipative model (vortices occur during the critical regime of phase transitions). The null spike appears in the band pass filtered brown noise activity and can be conceived as a *shutter* that blanks the intrinsic background ECoG. When the order parameter goes to zero the microscopic activity (of the background state) does not decrease but, consistently with the model description, it becomes disordered (fully symmetric). In such a state of very low analytic amplitude, the analytic phase is undefined, as it is indeed at the center line of the vortex core, and the system, under the incoming weak sensory input, may re-set the background activity in a new AM frame, if any, formed by reorganizing the existing activity. The analytic amplitude decrease repeats in the theta or alpha range, independently of the repetitive sampling of the environment by limbic input. Consistently with observations, in the dissipative model the reduction in activity constitutes a singularity in the dynamics at which the phase is undefined. The aperiodic shutter allows opportunities for phase transitions.

Imploding and exploding regime of the phase cone

In the phase transition processes occurring in a finite span of time, in which the formation of defects (e.g. vortices) occurs, a maximally stable new configuration is attained after a certain lapse of time since the transition has started. The system is said to be in the critical or Ginzburg regime during such a lapse of time. Reliable information on the critical regime behavior is provided by using the harmonic approximation for the evolution of the space-time dependent order parameter v [62, 53, 54]. By resorting to such an approximation, we expand the v field into partial waves:

$$v(x,t) = \sum_{\mathbf{k}} \{u_{\mathbf{k}}(t)e^{i\mathbf{k}\cdot\mathbf{x}} + u^{\dagger}_{\mathbf{k}}(t)e^{-i\mathbf{k}\cdot\mathbf{x}}\} \ . \tag{15}$$

Here we omit the dependence on temperature since this does not affect our discussion. In the Ginzburg-Landau (GL) formalism, for each k-mode ($k \equiv \sqrt{\mathbf{k}^2}$), the equations for the parametric oscillators $u_{\mathbf{k}}$ is [63] (see also [53, 54]):

$$\ddot{u}_{\mathbf{k}}\,(t) + (\mathbf{k}^2 - m^2)\,u_{\mathbf{k}} = 0 \ . \tag{16}$$

The oscillator frequency is

$$M_k(t) \ = \ \sqrt{\mathbf{k}^2 - m^2(t)}, \tag{17}$$

In full generality, we are assuming that m^2 may depend on time. At each t, $M_k(t)$ is real for each k provided, during the critical regime time interval, it is

$$\mathbf{k}^2 \geq m^2(t) \ , \tag{18}$$

for each k-mode. This turns out to be a condition on the k-modes propagation. Let $t = 0$ and $t = \tau$ denote the times at which the critical regime starts and ends, respectively. For a given $\mathbf{k}$, Eq. (18) holds up to a time τ_k after which $m^2(t)$, for $t > \tau_k$, is larger than $\mathbf{k}^2$. The corresponding k-mode can propagate in a span of time $0 \leq \ t \ \leq \tau_k$. Therefore, the "effective

causal horizon" [64, 65] can happen to be inside the system (possible formation of more than a domain) or outside (single domain formation) according to whether the time occurring for reaching the boundaries of the system is longer or shorter than the allowed propagation time. This determines the dimensions to which the domains can expand. The explicit form of $m^2(t)$ determines the value of τ_k.

The time dependence of $m(t)$ may be modeled in a way to allow defect (i.e. vortex) formation [54]. We put:

$$m^2(t) = m_0^2 \, e^{2h(t)} \ , \tag{19}$$

where the function $h(t)$ has to be chosen in a specific model. The correlation propagation time is given by:

$$h(\tau_k) = \ln\left(\frac{k}{m_0}\right) \ \propto \ \ln\left(\frac{L}{\xi}\right) \ , \tag{20}$$

where ξ is the correlation length corresponding to the k-mode propagation and $L \propto m_0^{-1}$. L acts as an intrinsic infrared cut-off. Due to Eq. (18), small k values are excluded by the non-zero minimum value of $m^2(t)$. Long wave-lengths are thus precluded, which means that only domains of finite size can be obtained. At the end of the critical regime the correlation may extend over domains of linear size of the order of $\lambda_k \propto m^{-1}(\tau)$. $h(\tau_k)$ resembles the commonly called string tension [65].

In order to further specify our model, the explicit analytic expression for $h(t)$ is chosen to be [54]:

$$h(t) = \pm \frac{at}{bt^2 + c} \ , \tag{21}$$

where a, b, c are (positive) arbitrary parameters. We put $c/a\lambda \equiv \tau_Q$, $a\lambda/b \equiv \tau_0$, with λ an arbitrary constant. Note that $h(\tau_Q) = h(\tau_0)$. The time derivative of $h(t)$, and thus of $m^2(t)$, is zero at $t = \tau = \pm\sqrt{\tau_Q \tau_0}$. τ thus plays the role of the equilibrium time scale. We observe that

$$h(t) = \pm \frac{1}{\lambda\tau_Q} \frac{1}{1 + \frac{t^2}{\tau^2}} \ t \approx \pm \frac{\Gamma}{2} \ t \ , \tag{22}$$

for $t^2/\tau^2 \approx 1$, with $\Gamma \equiv 1/\lambda\tau_Q$. Since the size of the vortex core is given by $(m(t))^{-1}$, Eqs. (19) and (22) show that such a size evolves in time as $e^{\mp\Gamma \ t}$, $t < \tau$ ($t < \tau_k$ for the k-mode). This means that we have converging (imploding) and diverging (exploding) regimes, as indeed found in laboratory observations of the phase cone behaviors. We remark that Eq. (22) shows that the $\pm$ signs in Eq. (21) amount to working with both elements of the basis $(e^{+\Gamma/2 \ t}, e^{-\Gamma/2 \ t})$, as indeed required by mathematical correctness. In this sense, the $\pm$ double sign cannot be avoided in the model choice of $h(t)$. From a physical point of view, it is equivalent to working with time evolution pointing in one given time direction (say the $t > 0$ arrow of time) and with its "time-reversed" copy or image. This is perfectly consistent with one of the main features of the dissipative model where time-reversed excitations are introduced, thus "doubling" the system degrees of freedom. Moreover, in ref. [66] clockwise and counterclockwise (loop and anti–loop) rotations have been shown to be related by time–reversal transformations.

We observe that since the disordered ("normal") state is confined to the vortex core, in the imploding regime (the shrinking of the vortex core) long range correlation, i.e. ordering, is prevailing (the vortex is "squeezed out"); in the exploding regime (enlargement of the vortex core), local correlations (disorder) prevail.

Finally, the number of defects (of vortices) n_{def} possibly appearing during the critical regime is given in the linear approximation by [54, 65]:

$$n_{def} \propto m^2(\tau) \approx m_0^2 \ |\tau/\lambda\tau_Q| \ . \tag{23}$$

In conclusion, in the process of non-instantaneous phase transitions (as those observed in brain) the dissipative model predicts the existence of a vortex singularity associated (at the vortex core) with the abrupt decrease (null spike) of the order parameter (the analytic amplitude) and the concomitant increase of spatial variance of the phase field (the analytic phase). The resulting phase cones present both phase gradients, the positive and the negative one, as in the observations. The formation of imploding and exploding phase cones is shown to be allowed, as indeed deduced from observations.

Let us close this Section with a final comment. We have seen that coherent states play a relevant role in the dissipative many-body model. For example, the transformation (11) induces boson condensation and generates a (Glauber) coherent state. In ref. [67] it has been discussed the self-similarity property of coherent states in connection with fractal self-similarity property [68, 69]. The dissipative model thus predicts self-similarity as a characterizing property of brain dynamics [67, 70]. As observed in the previous Sections, laboratory observations show indeed that brain background activity is characterized by self-similarity. Measurements of the durations, recurrence intervals and diameters of neocortical EEG phase patterns have power-law distributions with no detectable minima. The power spectral densities in time and space of ECoGs from surface arrays conform to power-law distributions [23, 21, 71, 72, 73]. This suggests that the activity patterns generated by neocortical neuropil might be scale-free [74, 75, 76] with self-similarity in ECoGs patterns over distances ranging from hypercolumns to an entire cerebral hemisphere [34].

6. Conclusions

The discussion presented in this paper leads us to conclude that the crucial step in perception is the transition from the excited microscopic assembly to the large-scale mesoscopic AM pattern. That possibility occurs when a null spike (Fig. 10, D) of the necessary depth (Fig. 11, D) supervenes in the appropriate frequency range, and the order parameter manifested in the ECoG vanishes. Any pre-existing dissipative structure dissolves, leaving the microscopic neurons in maximal disorder, which is a state of symmetry. The null spike sets the conditions allowing spontaneous breakdown of symmetry, which opens the possibility for the activated assembly to capture the population by directing the trajectory into its basin of attraction. The precise location of the phase transition in time, space and spectrum vary randomly (Fig. 3, Fig. 10). When the null spike terminates and the order parameter returns, it sustains the new self-organized dissipative structure. The stability of the AM pattern is enhanced by the vortex (Fig. 5) that is frozen into the conic phase gradient (Fig. 4).

These basic features have been described by the dissipative many-body model. Several predictions have been derived and compared with experiments. It can be useful to list few of these experimentally confirmed model predictions. As already mentioned, the dissipative many-body model accounts for the observed dynamical formation of spatially extended domains of neuronal synchronized oscillations and of their rapid sequencing. The model explains indeed two main features of the ECoG data:

- the textured patterns of AM in distinct frequency bands correlated with categories of conditioned stimuli, i.e. *coexistence* of physically distinct AM patterns, and
- the remarkably rapid onset of AM patterns into (irreversible) sequences that resemble cinematographic frames.

Each spatial AM pattern is described to be consequent to spontaneous breakdown of symmetry triggered by external stimulus and is associated with one of the emerging unitarily inequivalent ground states. Their sequencing is associated to the non-unitary time evolution implied by dissipation. Moreover, consistently with experimental observations the model predicts that [6, 34]

- very low energy is required to excite AM correlated neuronal patterns,

- AM patterns have large diameters, with respect to the small sizes of the component neurons,
- duration, size and power of AM patterns are decreasing functions of their carrier wave number
- there is lack of invariance of AM patterns with invariant stimuli.
- there is heat dissipation at (almost) constant in time temperature (see also [6, 34]),
- null spikes occur in the process of phase transitions and the whole behavior of phase gradients and phase singularities in the vortices formation agrees with observations,
- that the phase field is constant within the frames,
- the insurgence of a phase singularity is associated with the abrupt decrease of the order parameter and the concomitant increase of spatial variance of the phase field,
- the onsets of vortices occurs *between* frames, not *within* them,
- the phase cones occur with random variation of sign (implosive and explosive) at the apex,
- that the phase cone apices occur at random spatial locations,
- that the apex is never initiated *within* frames, but *between* frames (during phase transitions).

The model leads to the classicality (not derived as the classical limit, but as a dynamical output) of functionally self-regulated and self-organized background activity of the brain.

Finally, self-similarity and scale-free dynamics suggested by observation finds its correspondence in the coherent state structure of brain dynamics as described by the model.

Acknowledgments
The authors express their appreciation for programming by Brian C. Burke and William Redfearn.

References

[1] von Neumann J 1958 *The Computer and the Brain* (New Haven CT: Yale UP)
[2] Freeman W J 2007 *Intentionality. Entry for Encyclopedia for Computational Neuroscience* ed E Izhikevich http://www.scholarpedia.org/article/Intentionality
[3] Vitiello G. 2001 *My Double Unveiled* (Amsterdam: John Benjamins).
[4] Freeman W J, Erwin H 2008 *Freeman K-set. Entry for Encyclopedia for Computational Neuroscience* ed E Izhikevich
http : //www.scholarpedia.org/article/Freeman_K − set
[5] Principe J C, Tavares V G, Harris J G and Freeman W J 2001 *Proceedings IEEE* **89** 1030
[6] Freeman W J, Vitiello G 2008 *J. Phys. A: Math. Theor.* **41** 304042
http://Select.iop.org, q-bio.NC/0701053v1.
[7] Lashley K 1948 *The Mechanism of Vision, XVIII, Effects of Destroying the Visual "Associative Areas" of the Monkey* (Provincetown MA:Journal Press)
[8] Freeman W J 2001 *How Brains Make Up Their Minds* (New York: Columbia UP)
[9] Freeman W J, Baird B 1987 *Behavioral Neuroscience* **101** 393
[10] Freeman W J 1979 *Biol Cybern* **33** 237
[11] Freeman W J 1975/2004 *Mass Action in the Nervous System* (New York: Academic Press)
[12] Freeman W J 2007 *Scale-free neocortical dynamics. Encyclopedia for Computational Neuroscience* ed E Izhikevich
http : //www.scholarpedia.org/article/Scale − free_neocortical_dynamics
[13] Freeman W J, Burke B C, Holmes M D 2003 *Human Brain Mapping* **19** 248
[14] Freeman W J 2006 *Clin. Neurophysiol* **117** 572
http://repositories.cdlib.org/postprints/1480/
[15] Freeman W J, O'Nuillain S, Rodriguez J 2008 *J Integr Neurosci* **7** 337
[16] Schroeder M 1991 *Fractals, Chaos, Power Laws* (San Francisco: WH Freeman)
[17] Freeman W J, Zhai J 2008 *Cognitive Neurodynamics* **3** in press
[18] Freeman W J, Kozma R, Bollobás B, Riordan O 2009 Scale-Free Cortical planar Graphs in *Handbook of Large-Scale Random Networks. Bolyai-Springer Series on Advanced Combinatorics* ch 7 ed B Bollobás, R Kozma, D Mikls (New York: Springer)
[19] Rice S O 1950 *Mathematical Analysis of Random Noise - and Appendixes. Technical Publications Monograph B-1589* (New York: Bell Telephone Labs Inc)
[20] Freeman W J 2009 *Cognitive Neurodynamics* **3** in press.

[21] Freeman W J 2004 *Clin. Neurophysiol.* **115** 2089
http://repositories.cdlib.org/postprints/1486
[22] Pikovsky A, Rosenblum M, Kurths J. 2001 *Synchronization - A Universal Concept in Non-linear Sciences* (Cambridge UK: Cambridge UP)
[23] Freeman W J 2004 *Clin. Neurophysiol.* **115** 2077
[24] Freeman W J 2007 *Hilbert transform for brain waves. Entry for Encyclopedia for Computational Neuroscience* ed E Izhikevich $http://www.scholarpedia.org/article/Hilbert\_transform\_forbrain\_waves$
[25] Freeman W J 2005 *Clin. Neurophysiol.* **116** 1118
http://authors.elsevier.com/sd/article/S1388245705000064 http://repositories.cdlib.org/postprints/2134/
[26] Ricciardi L M, Umezawa H 1967 *Kibernetik* **4** 44; Reprint in *Brain and Being* 2004 eds G G Globus, K H Pribram, G Vitiello (Amsterdam: John Benjamins) p 255
[27] Stuart C I J, Takahashi Y, Umezawa H 1978 *J.Theor. Biol.* **71** 605
[28] Stuart C I J, Takahashi Y, Umezawa H 1979 *Found. Phys.* **9** 301
[29] Del Giudice E, Doglia S, Milani M, Vitiello G 1985 *Nucl. Phys.* B **251** (FS 13) 375
[30] Del Giudice E, Doglia S, Milani M, Vitiello G 1986 *Nucl. Phys.* B **275** (FS 17) 185
[31] Del Giudice E, Preparata G, Vitiello G 1988 *Phys. Rev. Lett.* **61** 1085
[32] Celeghini E, Rasetti M, Vitiello G 1992 *Annals of Phys.* **215** 156
[33] Vitiello G 1995 *Int. J. Mod. Phys.* B **9** 973
[34] Freeman W J and Vitiello G 2006 *Phys. of Life Reviews* **3** 93
http://www.arxiv.org/find [Freeman]; q-bio.OT/0511037
[35] Freeman W J and Vitiello G 2008 Vortices in brain waves, Forthcoming
[36] Hopfield J J 1982 *Proc. of Nat. Acad. Sc. USA* **79** 2554
[37] Amit D J 1989 *Modeling Brain Function: The World of Attractor Neural Networks* (Cambridge UK: Cambridge University Press)
[38] Mezard M, Parisi G, Virasoro M, 1987 *Spin glass theory and beyond* (Singapore: World Sci.)
[39] Schrödinger E, 1944. *What is life?* [1967 reprint] (Cambridge: Cambridge University Press)
[40] Sivakami S and Srinivasan V 1983 *J. Theor. Biol.* **102** 287
[41] Freeman W J, Burke B C, Holmes M D 2003 *Human Brain Mapping* **19** 248
[42] Freeman W J, Burke B C, Holmes M D, Vanhatalo S 2003 *Clin. Neurophysiol.* **114** 1055
[43] Jibu M and Yasue K 1992 *Cybernetics and System Research* ed R Trappl (Singapore: World Scientific) p 797
[44] Jibu M and Yasue K 1995 *Quantum brain dynamics and consciousness* (Amsterdam: John Benjamins)
[45] Jibu M, Pribram K H, Yasue K 1996 *Int. J. Mod. Phys.* B **10** 1735
[46] Haider B, Duque A, Hasenstaub A R, McCormick D A 2006 *J. Neurosci.* **26**, 4535
[47] Peterson C C, Hahn T T G, Mehta M, Grinvald A, Sakmann B 2003 *Proc. Natl. Acad. Sci. U.S.A.* **100** 13638
[48] Raichle M E 2006 *Science* **314** 1249
[49] Stapp H P 1993/2003 *Mind, matter an quantum mechanics* (New York: Springer-Verlag)
[50] Hameroff S, Penrose R 1996 *J. Conscious. Stud.* **3** 36
[51] Penrose R 1994 *Shadows of the mind* (Oxford: Oxford University Press)
[52] Alfinito E and Vitiello G 2000 *Int. J. Mod. Phys.* B **14** 853 [Erratum 2000 ibid. B **14** 1613].
[53] Alfinito E, Romei O, Vitiello G 2002 *Mod. Phys. Lett.* B **16** 93
[54] Alfinito E and Vitiello G 2002 *Phys. Rev.* B **65** 054105
[55] Vitiello G 2004 *Int. J. Mod. Phys.* B **18** 785
[56] Pessa E and Vitiello G 2003 *Mind and Matter* **1** 59
[57] Pessa E and Vitiello G 2004 *Int. J. Mod. Phys.* B **18** 841
[58] Matsumoto H, Papastamatiou N J, Umezawa H, Vitiello G 1975 *Nucl. Phys.* B **97** 61
Matsumoto H, Papastamatiou N J, Umezawa H 1975 *Nucl. Phys.* B **97** 90
[59] Umezawa H 1993 *Advanced field theory: micro, macro and thermal concepts* (New York: AIP)
[60] Anderson P W 1984 *Basic Notions of Condensed Matter Physics* (Menlo Park: Benjamin)
[61] Higgs P 1996 *Phys. Rev.* **145** 1156
Kibble T W B 1967 *Phys. Rev.* **155** 1554
[62] Bettencourt L M A, Antunes N A, Zurek W H 2000 *Phys. Rev.* D **62** 065005
Antunes N A, Bettencourt L M A, Zurek W H 2000 *Phys. Rev. Lett.* **82** 2824
[63] Perelomov A M 1986 *Generalized Coherent States and their Applications* (Berlin: Springer)
[64] Kibble T W B 2000 in *Topological defects and the non-equilibrium dynamics of symmetry breaking phase transitions. NATO Science Series C 549* ed Y M Bunkov and H Godfrin (Dordrecht: Kluwer Acad) p 7
Volovik G E 2000 in *Topological defects and the non-equilibrium dynamics of symmetry breaking phase transitions. NATO Science Series C 549* ed Y M Bunkov and H Godfrin (Dordrecht: Kluwer Acad) p 353.
[65] Zurek W H 1997 *Phys. Rep.* **276** 177 and refs. therein quoted.

[66] Alfinito E, Vitiello G 2003 *Mod. Phys. Lett.* B **17** 1207
[67] Vitiello G 2009 *New Mathematics and Natural Computation* in print
[68] Peitgen H O, Jürgens H, Saupe D 1986 *Chaos and fractals. New frontiers of Science* (Berlin: Springer-Verlag)
[69] Bunde A and Havlin S 1995 (Eds.) *Fractals in Science* (Berlin: Springer-Verlag)
[70] Vitiello G 2009 Fractals and the Fock-Bargmann representation of coherent states, in print
[71] Braitenberg V, Schüz A 1991 *Anatomy of the Cortex: Statistics and Geometry* (Berlin: Springer-Verlag)
[72] Linkenkaer-Hansen K, Nikouline V M, Palva J M, Iimoniemi R J 2001 *J Neurosci* **15** 1370
[73] Hwa R C, Ferree T 2002 *Phys. Rev.* E **66** 021901
[74] Wang X F and Chen G R 2003 *IEEE Trans. Circuits Syst.* **31** 6
[75] Freeman W J 2005 *J. Integrative Neuroscience* **4** 407
[76] Bassett D S, Meyer-Lindenberg A, Achard S, Duke T and Bullmore E 2006 *Proc. Natl. Acad. Sci. U.S.A.* **103** 19518